

Niche-based screening identifies small-molecule inhibitors of leukemia stem cells

Kimberly A Hartwell^{1-3,13}, Peter G Miller^{2,3,13}, Siddhartha Mukherjee^{4,12}, Alissa R Kahn⁵, Alison L Stewart¹, David J Logan¹, Joseph M Negri¹, Mildred Duvet^{1,4}, Marcus Järås², Rishi Puram^{2,3}, Vlado Dancik¹, Fatima Al-Shahrour^{1,2}, Thomas Kindler², Zuzana Tothova^{2,3}, Shrikanta Chattopadhyay^{1,6}, Thomas Hasaka¹, Rajiv Narayan¹, Mingji Dai^{1,7}, Christina Huang¹, Sebastian Shterental², Lisa P Chu², J Erika Haydu², Jae Hung Shieh⁵, David P Steensma^{3,8}, Benito Munoz¹, Joshua A Bittker¹, Alykhan F Shamji¹, Paul A Clemons¹, Nicola J Tolliday¹, Anne E Carpenter¹, D Gary Gilliland^{1,2,8,9,12}, Andrew M Stern^{1,12}, Malcolm A S Moore^{10*}, David T Scadden^{1,4,6*}, Stuart L Schreiber^{1,7,9*}, Benjamin L Ebert^{1-3,8*} & Todd R Golub^{1,3,9,11*}

Efforts to develop more effective therapies for acute leukemia may benefit from high-throughput screening systems that reflect the complex physiology of the disease, including leukemia stem cells (LSCs) and supportive interactions with the bone marrow microenvironment. The therapeutic targeting of LSCs is challenging because LSCs are highly similar to normal hematopoietic stem and progenitor cells (HSPCs) and are protected by stromal cells *in vivo*. We screened 14,718 compounds in a leukemia-stroma co-culture system for inhibition of cobblestone formation, a cellular behavior associated with stem-cell function. Among those compounds that inhibited malignant cells but spared HSPCs was the cholesterol-lowering drug lovastatin. Lovastatin showed anti-LSC activity *in vitro* and in an *in vivo* bone marrow transplantation model. Mechanistic studies demonstrated that the effect was on target, via inhibition of HMG-CoA reductase. These results illustrate the power of merging physiologically relevant models with high-throughput screening.

The hematopoietic niche is a complex mixture of heterogeneous cell types that supports normal hematopoiesis and is hypothesized to have a chemoprotective role in the treatment of acute myeloid leukemia (AML), possibly contributing to the failure of standard-of-care chemotherapy to cure at least half of adult patients with this disease¹⁻³. Within AML is a population of cells with the capacity for self-renewal, disease initiation and disease propagation termed LSCs⁴. These cells are less sensitive to mainstay AML chemotherapies such as daunorubicin and cytarabine^{5,6} and are particularly responsive to a number of supportive stromal factors, including interleukin-6 (IL-6), stromal cell-derived factor-1, IL-8 and angiopoietin-1 (refs. 3,7), further blunting the cytotoxic effects of chemotherapy.

Strategies to target LSC dependencies within the context of the bone marrow microenvironment are therefore attractive; however, two major obstacles have made such therapeutic targeting challenging in practice. First, many of the liabilities identified to date in leukemia cells also exist in normal HSPCs owing to the biological similarity of these populations^{1,8}. Illustrating this, the dose-limiting

toxicity for standard-of-care AML treatments, including cytarabine and daunorubicin, is toxicity to normal HSPCs^{9,10}. As such, discovering therapeutics that target LSCs but spare HSPCs is difficult. Second, to date there has not been a way to model complex phenotypes of primary leukemia cells within the bone marrow niche in a manner compatible with high-throughput small-molecule screening. Such screening requires that cells be grown in microtiter plates with a reproducible, automated readout. This is particularly problematic in the case of LSCs and HSPCs, whose stem-associated properties are recognized *ex vivo* via the formation of 'cobblestone areas' (the burrowing of primitive cells beneath a layer of stromal fibroblasts, forming phase dark areas of cobblestone area-forming cells (CAFCs) organized in tight association), which generally require a highly trained eye to detect microscopically by phase contrast¹¹⁻¹³.

We reasoned that a high-throughput screening system capable of supporting primary cells in the context of a simulated bone marrow niche might enable the discovery of leukemia-selective compounds not otherwise identified using standard cell line-based

¹Broad Institute, Cambridge, Massachusetts, USA. ²Department of Medicine, Division of Hematology, Brigham and Women's Hospital and Harvard Medical School, Boston, Massachusetts, USA. ³Harvard Medical School, Boston, Massachusetts, USA. ⁴Center for Regenerative Medicine and Cancer Center, Massachusetts General Hospital, Boston, Massachusetts, USA. ⁵Department of Pediatrics, Memorial Sloan-Kettering Cancer Center, New York, New York, USA. ⁶Department of Stem Cell and Regenerative Biology, Harvard University, Cambridge, Massachusetts, USA. ⁷Department of Chemistry and Chemical Biology, Harvard University, Cambridge, Massachusetts, USA. ⁸Department of Medical Oncology, Dana-Farber Cancer Institute, Harvard Medical School, Boston, Massachusetts, USA. ⁹Howard Hughes Medical Institute, Harvard Medical School, Chevy Chase, Maryland, USA. ¹⁰Cell Biology Program, Memorial Sloan-Kettering Cancer Center, New York, New York, USA. ¹¹Department of Pediatric Oncology, Dana-Farber Cancer Institute, Boston, Massachusetts, USA. ¹²Present addresses: Department of Medicine and Irving Cancer Research Center, Columbia University School of Medicine, New York, New York, USA (S.M.); Penn Medicine, Philadelphia, Pennsylvania, USA (D.G.G.); Department of Computational and Systems Biology, University of Pittsburgh Drug Discovery Institute, Pittsburgh, Pennsylvania, USA (A.M.S.). ¹³These authors contributed equally to this work.

*e-mail: m-moore@ski.mskcc.org, dscadden@mgh.harvard.edu, stuart_schreiber@harvard.edu, bebert@partners.org or golub@broadinstitute.org

viability screens. We report here the development of such a system involving the co-culture of primary LSC-enriched cells with bone marrow stromal cells coupled to an automated machine-learning algorithm capable of recognizing the CAFC phenotype. A small-molecule screen identified new compounds that inhibited leukemic CAFCs while sparing normal HSPCs as well as compounds previously established as LSC selective. A subset of the compounds identified were not readily apparent by traditional cell-line screening, illustrating the limitations of conventional methods. These experiments demonstrate the feasibility of physiologically relevant small-molecule screening within a niche-like microenvironment. Moreover, the panel of compounds identified may represent starting points for new types of AML therapies.

RESULTS

Sustaining primary leukemia in a niche-like environment

To generate primary leukemia cells for high-throughput study, we used a well-characterized mouse model of human AML driven by the oncogene *MLL-AF9* (refs. 3,8,14). The LSC-enriched fraction of cells (hereafter referred to as 'LSCe cells') was isolated from the bone marrow of leukemic animals by fluorescence-activated cell sorting (FACS) (Supplementary Results, Supplementary Fig. 1a,b and Online Methods). Notably, as LSCe cells are difficult to maintain over extended periods *in vitro* when cultured in isolation⁸, we developed a co-culture system to support these cells *ex vivo* and to enable cobblestone area formation. Historically, *ex vivo* maintenance of normal HSCs has required co-culture with supportive stroma, and stem-cell activity has been most faithfully quantified *ex vivo* by cobblestone area formation in the CAFC assay or by colonies arising from cobblestone areas in the long-term culture-initiating cell assay^{12,13}. Primary leukemia cells have similarly been examined¹¹; however, these assays have not been attempted on a high-throughput scale. Toward that goal, we plated dsRed⁺ LSCe cells in 384-well format onto two types of supportive GFP⁺ bone

marrow-derived stromal cells to identify reproducible effects: primary bone marrow mesenchymal stromal cells derived from actin-GFP mice or GFP-expressing bone marrow stroma-derived OP9 cells (Online Methods).

LSCe cells co-cultured with either stroma grew robustly in the absence of cytokine supplementation, forming distinct cellular aggregates beneath the stroma, indicative of cobblestone area formation (Fig. 1a). Moreover, cell culture medium that had been pre-conditioned by OP9 stromal cells for 3 d augmented cobblestone area formation beneath this type of stromal monolayer, suggesting that secreted factors contribute to the CAFC phenotype. We also found that the enrichment for stem cell activity using c-Kit^{hi} cells produced higher frequencies of CAFCs, as predicted, relative to c-Kit^{lo} cells seeded at the same density (Supplementary Fig. 1c and Online Methods). To affirm the *in vivo* leukemia-initiating potential of the LSCe cells in our model, we co-cultured 25, 100 or 500 LSCe cells with bone marrow stromal cells and transplanted the contents into lethally irradiated mice 6 d later. All of the recipient animals developed leukemia within 30 d, indicating the intrinsic leukemogenicity of the LSCe cells and its persistence in the high-throughput co-culture system (Supplementary Fig. 1d).

To enable high-throughput studies, we also developed an image analysis pipeline by incorporating CellProfiler software¹⁵ to enumerate the CAFC phenotype in the dsRed channel based on the most discriminating morphological features of the CAFCs. The machine-learning algorithm¹⁶ used several hundred manually selected examples of CAFC and non-CAFC cell images to generate a set of 50 morphological 'rules' (for example, shape, intensity, texture and cell-neighbor relationships) that defined CAFCs (Fig. 1b, Supplementary Table 1, Supplementary Fig. 1e and Online Methods). Tests on an independent set of images indicated an accuracy sufficient for screening, with a sensitivity of 86% and a specificity of 87% compared to manual review by experts (Online Methods).

Figure 1 | A high-throughput system for probing LSCe cells within a stromal niche.

(a) LSCe cells generate CAFC (arrows) and non-CAFC morphologies when plated with bone marrow stroma (left, primary BMSCs; right, OP9 cells) at the 6-d assay endpoint. Qualitative images are shown as a visual introduction to the devised assay. The red channel has been pseudocolored to accommodate colorblindness. Scale bars, 50 μ m. (b) A representative example of the 'number of neighbors' rule, 1 of 50 computational rules that together identify CAFCs. A raw image of LSCe cells in co-culture (left, dsRed channel) is converted to a heat map (middle) reflecting the number of adjacent cells (red, many; blue, few), identifying cell 'objects' (right; Online Methods) that are part of a cobblestone area (orange, CAFC; blue, non-CAFC). Qualitative images are shown as a conceptual introduction to the computational method. Scale bars, 50 μ m. (c) Schematic of the small-molecule co-culture screen protocol. (d) The co-culture screen data for 14,718 compounds (blue) added at \sim 5 μ M, in duplicate. Values were normalized to the means of both neutral (DMSO carrier, yellow, set at 0% effect) and positive (10 μ M XK469, a topoisomerase II β inhibitor, red, set at \sim 100% effect) controls. (e) Schematic summarizing the filtering steps used to define high-priority compounds. The number of compounds prioritized at each step is shown.

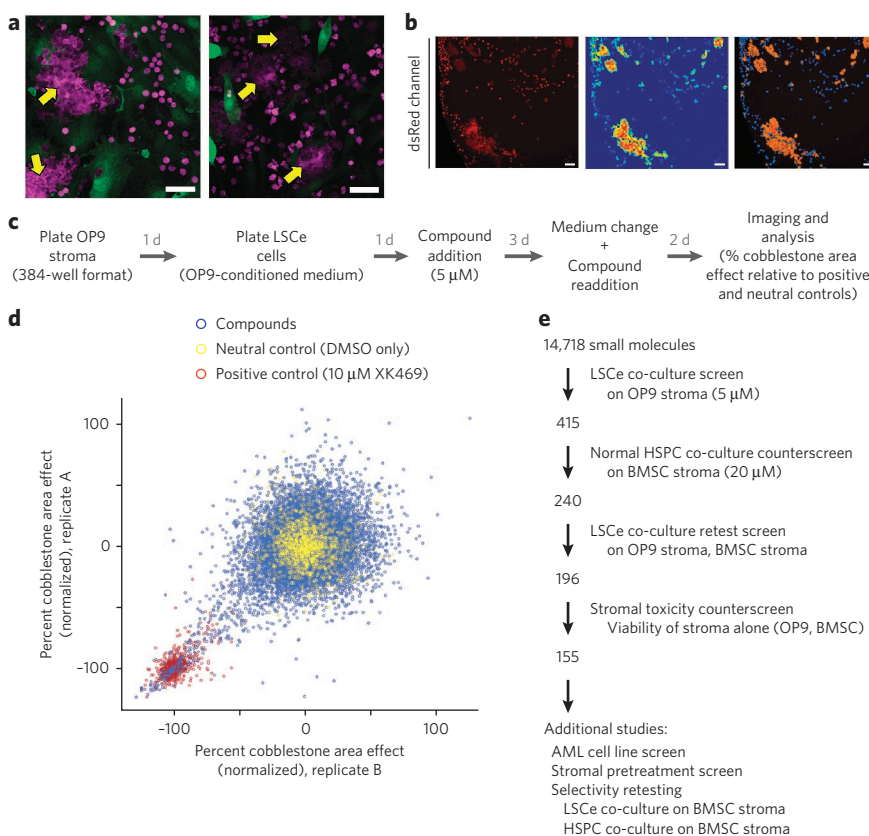
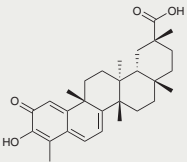
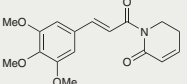
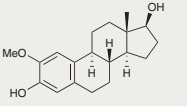
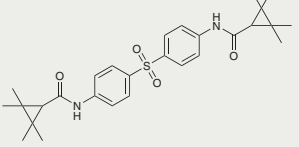
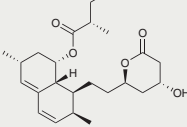
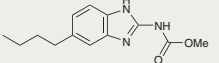
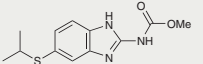
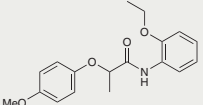
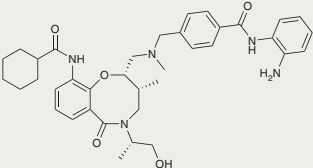
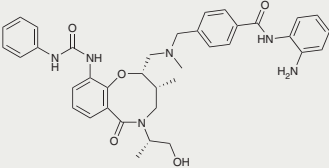
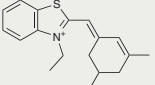
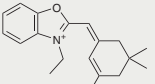
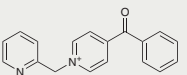
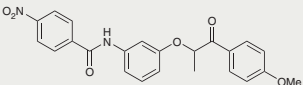
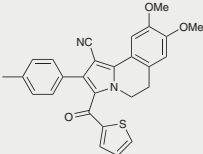


Table 1 | Prioritized screening hits display selective toxicity to LSCe cells relative to HSPCs in co-culture

Name	Structure	LSCe assay EC ₅₀ (nM)	HSPC assay EC ₅₀ (nM)
Celastrol (1)		100	1,300
Piperlongumine (2)		380	4,900
2-Methoxy estradiol (3)		62	>20,000
BRD7116 (4)		200	>20,000
Lovastatin (5)		170	>20,000
Parbendazole (6)		76	>20,000
Methiazole (7)		470	>20,000
BRD1686 (8)		1,400	>20,000
BRD9608 (9)		700	>20,000
BRD6708 (10)		2,100	>20,000
BRD1319 (11)		≤10	>20,000
BRD0638 (12)		≤10	>20,000
BRD1856 (13)		810	16,000

(continued)

Table 1 | Prioritized screening hits display selective toxicity to LSCe cells relative to HSPCs in co-culture (continued)

Name	Structure	LSCe assay EC ₅₀ (nM)	HSPC assay EC ₅₀ (nM)
BRD6491 (14)		240	>20,000
BRD8404 (15)		150	>20,000

The names and structures of 15 prioritized small-molecule screening hits are shown, with EC₅₀ values (from dose-response curves across eight concentrations) for both LSCe cells (as percent cobblestone area effect; two replicates per concentration) and HSPCs (as total cells per well; six replicates per concentration) co-cultured under identical conditions on primary BMSC stromal cells. Celestrol, piperlongumine and 2-methoxy estradiol were previously identified, validating the screening approach.

Small-molecule screening for leukemia selectivity

We screened 14,718 small-molecule compounds in duplicate, including ~1,920 bioactive molecules, 1,600 natural products and 2,880 compounds generated via diversity-oriented synthesis¹⁷ (Fig. 1c, Supplementary Table 2 and Online Methods) and determined that compounds inhibiting CAFCs by at least 85% were detected with 98% confidence (Supplementary Fig. 1f). Using this approach, we identified 415 compounds that inhibited leukemic CAFCs in co-culture (Fig. 1d and Online Methods).

We next excluded 145 of the 415 hits that caused gross stromal cell toxicity, killed normal HSPCs or both on the basis of data from a screen of the same compounds at ~20 μM on HSPCs (Lin^b Sca-1⁺ c-Kit⁺ CD48^b, from β-actin-dsRed mice) co-cultured with primary bone marrow stromal cells (Stewart, A.L., unpublished data; Online Methods).

We retested 240 of the remaining compounds in an eight-point dose response (from ~150 nM to 20 μM) on LSCe cells in co-culture with OP9 stromal cells and in co-culture with bone marrow stromal cells. In the presence of one of the stromal types, 196 compounds exhibited a dose response with a half-maximum effective concentration (EC₅₀) ≤ 5 μM, and 139 compounds displayed activity in the presence of both types (Online Methods). To exclude the possibility that CAFC inhibition was a result of direct stromal toxicity, we also tested the compounds in an eight-point dose on OP9 or bone marrow stromal cell monolayers in the absence of LSCe cells using a CellTiter-Glo viability readout. At concentrations below 20 μM, 36 compounds exhibited stromal toxicity (Supplementary Fig. 1g) and were excluded from further study. Together, these filters identified 155 prioritized compounds that inhibited LSCe cells relative to normal HSPCs and lacked toxicity to two bone marrow stromal cell types (Fig. 1e and Supplementary Table 3).

We more rigorously assessed the selectivity of the prioritized hits by examining the compounds at eight concentrations against both normal HSPCs and LSCe cells, each co-cultured on primary bone marrow stromal cells. A subset, prioritized on the basis of potency and selectivity, was subsequently re-examined (Online Methods). Several of these compounds displayed greater than 100-fold selectivity against leukemia cells compared to normal HSPCs (Table 1). Notably, compounds known to have preferential activity against LSCs, including celestrol (1), a triterpenoid antioxidant compound¹⁸, and parthenolide, a sesquiterpene lactone¹⁹, were among the 155 validated hits from the screen (Table 1 and Supplementary Table 3). Moreover, parthenolide is known to have activity against LSCs *in vivo*²⁰. We also identified 2-methoxy-estradiol (3), a microtubule inhibitor known to lack myelosuppressive side effects owing to its inability to bind the tubulin protein expressed in HSPCs²¹ (Table 1). These results indicate that the LSCe co-culture assay yields physiologically relevant insights and starting points for therapeutic discovery. Among the new compounds we identified were two benzimidazole carbamates,

parbendazole (6) and methiazole (7), used as anthelmintic agents in cattle feed (Table 1 and Supplementary Fig. 2a).

To determine whether the co-culture assay could reveal compounds not readily identified in standard screens of AML cell line viability, we tested the 155 compounds on six human AML cell lines (U937, THP-1, NOMO-1, SKM-1, NB4 and OCI-AML3), two of which (NOMO-1 and THP-1) harbor the *MLL-AF9* oncogene present in the primary leukemia cells used in our initial screen. We tested the compounds at eight concentrations in the absence of co-culturing using standard conditions and a viability readout (CellTiter-Glo). Whereas a subset of compounds, such as parbendazole and methiazole, also displayed potent activity in the AML cell lines (EC₅₀ < 0.625 μM for each of six cell lines; Supplementary Fig. 2b and Supplementary Table 3), other compounds showed greater than tenfold higher potency on primary LSCe cells in co-culture compared to their mean potency across the AML cell lines (Supplementary Table 3). We also identified compounds with greater activity against the cell lines than the co-cultured LSCe cells, indicating that primary LSCe cells are not merely nonspecifically more sensitive than established cell lines (Supplementary Table 3). As described below, we next selected two compounds for more extensive follow up because they illustrated the biology newly exposed by the screen: BRD7116 (4), a compound with cell-non-autonomous antileukemia activity, and lovastatin, a compound that would have been overlooked with conventional cell line-based screening.

BRD7116 displays cell-non-autonomous anti-leukemia activity

To identify compounds that inhibit LSCe cells via activity on the stromal cells (a property that would not be discoverable using standard cell line screening), we pretreated OP9 stroma at eight concentrations for 3 d, washed the stroma before the addition of LSCe cells and then imaged the co-cultures 6 d later (Supplementary Fig. 3a). We hypothesized that inhibition of cobblestone area formation under these conditions would be a result of compound activity on the stromal cells, as the LSCe cells were not directly exposed. All 155 of the hits were tested in this way. Troglitazone, a peroxisome proliferator-activated receptor-γ (PPAR-γ) agonist used for the treatment of diabetes²², inhibited leukemic CAFCs in the stromal pretreatment screen, yielding a dose-response curve similar to that observed in co-culture (Supplementary Fig. 3b). This inhibition was accompanied by a dose-dependent adipocytic change in the stroma (Supplementary Fig. 3c), consistent with the established ability of PPAR-γ agonists to regulate adipogenesis²³. OP9 stromal cells can readily differentiate into adipocytes²⁴, and adipocytes are known to antagonize hematopoietic cell self-renewal²⁵. Consistent with a cell-non-autonomous mechanism, none of the AML cell lines tested were sensitive to troglitazone at concentrations as high as 35 μM (Supplementary Fig. 3d).

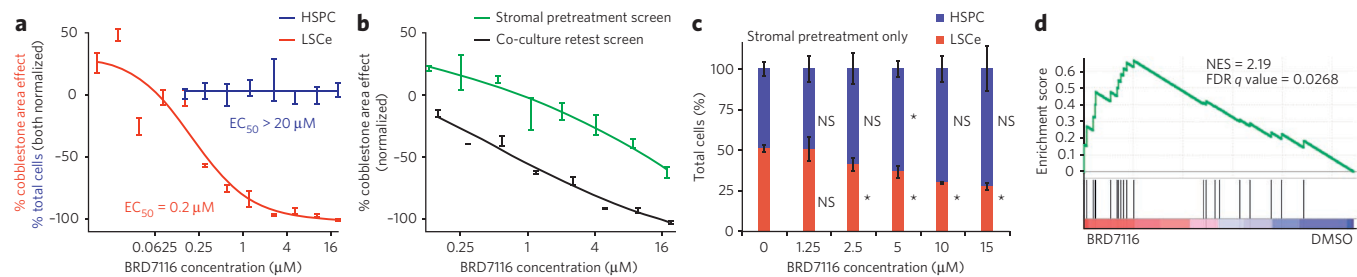


Figure 2 | New small molecule BRD7116 selectively targets LSCe cells by cell-autonomous and cell-non-autonomous mechanisms. (a) Dose-response effects of *bis*-aryl sulfone hit BRD7116 on LSCe cells (red, in duplicate) and normal HSPCs (blue, six replicates per dose) co-cultured on primary BMSC stroma, shown overlaid. BRD7116 was applied to the co-cultures in both cases. (b) The effects of treating only the stromal monolayer before co-culture are compared to the effects of treating both the stroma and LSCe cells together in co-culture. The data shown is from the stromal pretreatment secondary screen in which OP9 stromal cells were treated with BRD7116 for 3 d before LSCe cell plating (green). The LSCe co-culture retest data with OP9s (black) is also shown. Both screens were performed in duplicate. (c) The effects of treating only the stromal monolayer with BRD7116 for 3 d before the plating of admixed LSCe cells and HSPCs on primary BMSC stroma (as mean \pm s.e.m. of quadruplicate replicates). These two hematopoietic populations are quantified as the percentage of total hematopoietic cells under each stromal pretreatment condition. * $P < 0.05$; NS, not significant for effects relative to DMSO (0 μ M BRD7116) controls. (d) Compared to DMSO control, gene expression changes present in LSCe cells after 6 h of direct treatment with 5 μ M BRD7116 are significantly enriched for an AML differentiation gene signature, as defined by ATRA treatment of human AML cells by GSEA. NES, normalized enrichment score; FDR, false discovery rate.

A new compound, BRD7116, a *bis*-aryl sulfone, also showed evidence of stroma-mediated anti-LSCe activity. BRD7116 exhibited an EC_{50} of 200 nM for LSCe cells in co-culture (Fig. 2a), whereas it displayed limited activity against normal HSPCs (Fig. 2a) and AML cell lines (~50% inhibition at 20 μ M) (Supplementary Fig. 3e). BRD7116 also showed activity against patient-derived, primary human leukemia cells (Supplementary Fig. 3f). Furthermore, pretreatment of the stroma partially recapitulated the leukemic CAFC inhibition observed in co-culture (Fig. 2b) without evidence of altered stromal cell viability (CellTiter-Glo). In contrast to troglitazone, this niche effect was not accompanied by an obvious change in stromal morphology.

We next directly compared the relative inhibition of LSCe cells and HSPCs under internally controlled conditions using a three-component co-culture system. We added dsRed⁺ LSCe cells and GFP⁺ HSPCs (from ubiquitin C-GFP mice) simultaneously to uncolored bone marrow stromal cells pretreated for 3 d with BRD7116. In contrast to DMSO pretreatment controls, BRD7116 pretreatment

of the stroma preferentially inhibited the LSCe cells compared to HSPCs (Fig. 2c and Supplementary Fig. 3g).

Having observed a cell-non-autonomous effect, we next explored whether BRD7116 had any cell-autonomous effects on LSCe cells. We exposed LSCe cells for 6 h to 5 μ M BRD7116 in suspension and then performed gene-expression profiling. Using gene set enrichment analysis (GSEA)^{26,27}, we found that treatment of LSCe cells with BRD7116 induced transcriptional changes consistent with myeloid differentiation, as defined by all-*trans* retinoic acid (ATRA) treatment of ATRA-sensitive human AML cells²⁸ (Fig. 2d). The mechanism by which BRD7116 has this differentiation-inducing effect remains to be determined.

Lovastatin kills LSCs by HMG-CoA reductase inhibition

Lovastatin (5), a US Food and Drug Administration-approved drug in widespread clinical use for hypercholesterolemia, also emerged from the co-culture screen, inhibiting LSCe cobblestone area formation with an $EC_{50} < 200$ nM while showing limited activity against human

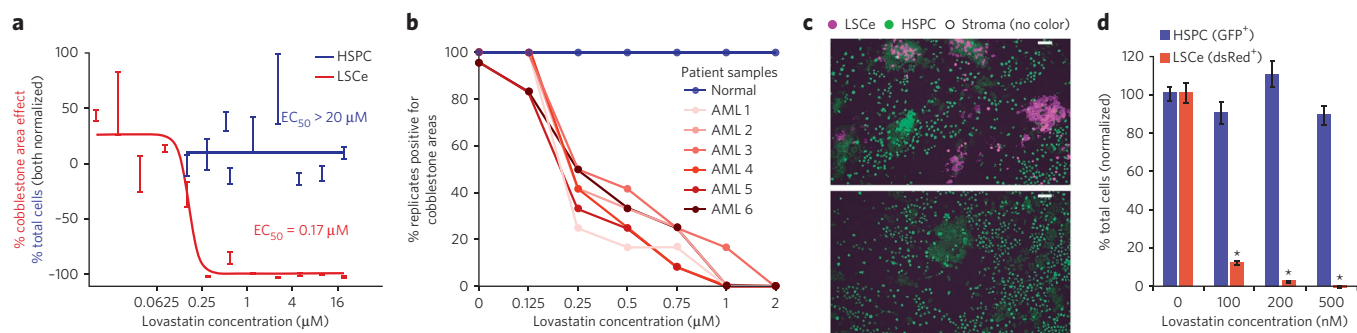


Figure 3 | Lovastatin selectively inhibits mouse and human leukemia cells in co-culture. (a) Lovastatin displays leukemia-selective activity (red dose-response curve, in duplicate) compared to HSPCs (blue, six replicates per dose) in co-culture with BMSCs. (b) The effects of lovastatin on CAFC activity of primary human CD34⁺ cells isolated from either normal or leukemic patient samples. Co-cultures were treated for 6 d and then rinsed. The fraction of replicate co-cultures containing cobblestone areas at the 5-week assay endpoint (2 weeks for the FLT3-ITD sample) is shown ($n \geq 6$). The clinical characteristics of the AML samples are as follows, including whether each AML case is primary (P) or directly related to previous cytotoxic therapy, as therapy-related (TR) leukemia is associated with a worse prognosis than *de novo* disease. AML 1: FLT3-ITD⁺ (P); AML 2: NPM1 mutation (P); AML 3: CBF β -MYH11 fusion (P); AML 4: trisomy 11, del(17p) (TR); AML5: CEPB α double mutation (P); AML 6: MLL-AF9 fusion (TR). (c) Representative images of admixed LSCe cells and HSPCs co-cultured with uncolored primary BMSCs at 5 d of exposure to DMSO (top) or 200 nM lovastatin (bottom). The red channel has been pseudocolored to accommodate colorblindness. Scale bars, 50 μ M. (d) Quantification of the effect (mean \pm s.e.m. of quadruplicate replicates) is also shown and is representative of two independent experiments. * $P < 0.001$ for LSCe cells relative to DMSO (0 μ M lovastatin) controls.

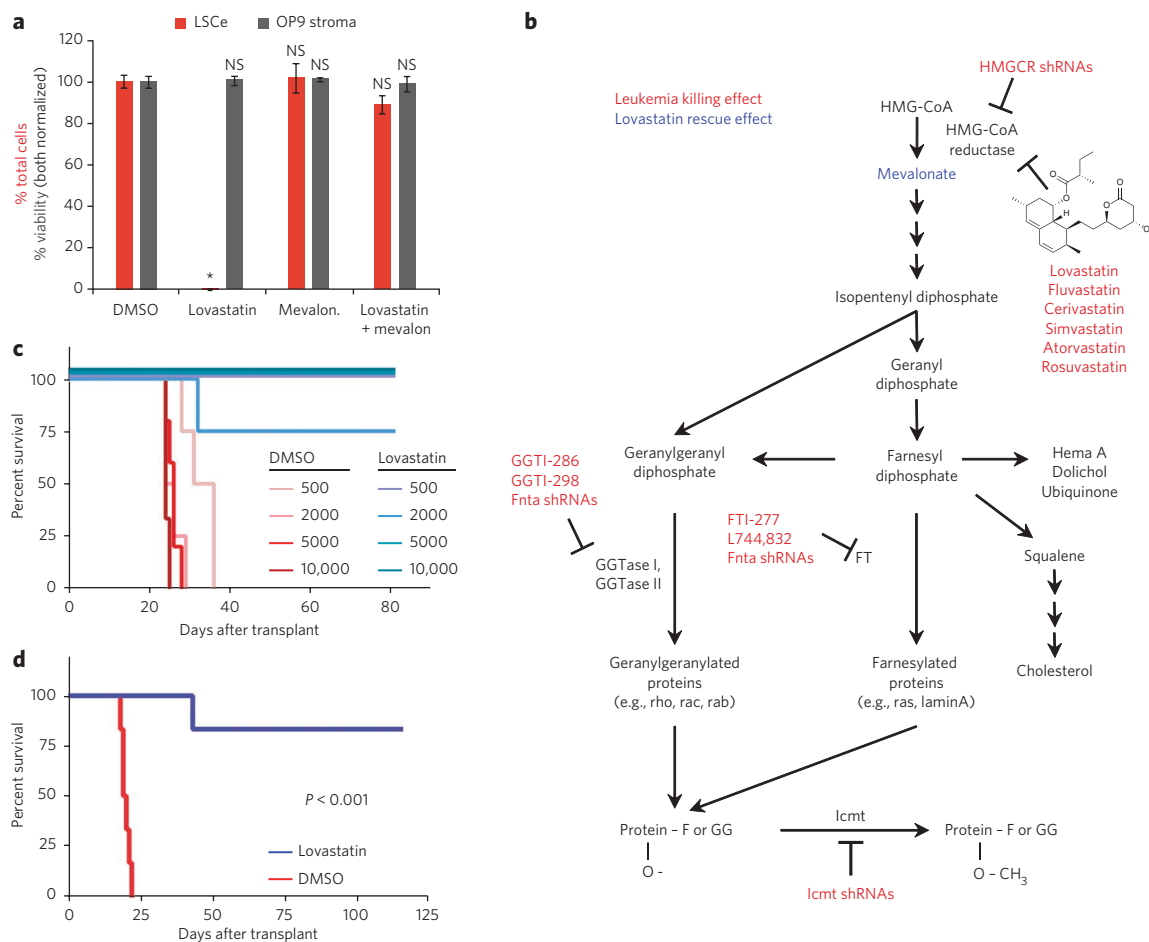


Figure 4 | Sensitivity of LSCe cells to HMGCR inhibition. (a) The addition of 2 mM mevalonate to co-cultures of LSCe cells with OP9 stroma rescued the anti-leukemia effect of 1 μ M lovastatin, with no stromal toxicity observed. Data are mean \pm s.e.m. of triplicate replicates and are representative of two independent experiments. *P* values shown are relative to DMSO control. **P* < 0.001; NS, not significant. (b) Schematic summarizing genetic and pharmacologic findings for the mevalonate pathway in LSCe cells *in vitro* (co-culture experiments) and *in vivo* (RNAi pooled screen). 'F' and 'GG' indicate farnesyl or geranylgeranyl moieties on target proteins ('protein'), respectively. (c) Limiting dilution analysis of varying numbers of LSCe cells pretreated in co-culture with BMSCs for 24 h with DMSO control or 5 μ M lovastatin before syngeneic transplantation into mice (*n* \geq 3, as shown). (d) *Ex vivo* treatment for 48 h with 5 μ M lovastatin impaired the ability of LSCe cells co-cultured with BMSCs to induce leukemia upon transplantation into mice relative to DMSO treatment (*n* = 6). Effects on admixed normal HSPCs are in **Supplementary Figure 5**.

and mouse AML cell lines (EC_{50} > 2,000 nM) and no apparent toxicity to normal HSPCs at concentrations as high as 20 μ M (Fig. 3a and **Supplementary Fig. 4a–c**). Of note, the inhibitory effects of lovastatin were cell autonomous, as lovastatin did not score in the stromal pretreatment assay described above. In addition, LSCe cells generated using an alternative oncogene, *MOZ-TIF2* (ref. 29), were also sensitive to lovastatin in co-culture (EC_{50} < 250 nM) (**Supplementary Fig. 4d**), indicating that the effect was not *MLL-AF9* specific.

We next extended the lovastatin studies to primary human leukemia cells, using longer-duration CAFC assays. CD34⁺ cells purified from umbilical cord blood or leukemic CD34⁺ cells purified from the bone marrow of leukemic patients^{11,12} were cultured together with stromal cells and treated for 6 d with lovastatin or DMSO and rinsed. Cobblestone area formation was assessed at 5 weeks (2 weeks for a leukemia harboring the *FLT3-ITD* oncogene³⁰). Lovastatin inhibited cobblestone area formation for all six patient-derived AML samples with potencies comparable to that seen in the mouse co-culture system, whereas no inhibition of normal HSPC cobblestone area formation was observed under these same conditions (Fig. 3b and **Supplementary Table 4**).

To directly compare the relative inhibition of LSCe cells and HSPCs under internally controlled conditions, we plated heterotypic

cultures consisting of dsRed⁺ LSCe cells, GFP⁺ HSPCs and uncolored primary BMSCs. We treated the co-cultures 24 h later with 200 nM lovastatin or DMSO and assessed them 5 d later. In contrast to control treatment with DMSO, lovastatin selectively inhibited the dsRed⁺ leukemia cells while sparing the GFP⁺ HSPCs, which continued to display normal, CAFC morphologies (Fig. 3c,d).

Statins act to lower cholesterol by inhibiting HMG-CoA reductase (HMGCR), the enzyme that catalyzes the rate-limiting step of cholesterol biosynthesis³¹. To evaluate the possibility that lovastatin was acting by an alternative mechanism, we tested the ability of mevalonate, the metabolite immediately downstream of HMGCR, to rescue the observed lovastatin effects. Consistent with an HMGCR on-target mechanism, mevalonate fully rescued the antileukemia effects of lovastatin in co-culture (Fig. 4a), and five additional statins (simvastatin, fluvastatin, cerivastatin, rosuvastatin and atorvastatin) selectively inhibited LSCe cells relative to normal HSPCs (**Supplementary Table 5**).

To further establish that the lovastatin effect was mediated by HMGCR inhibition, we next performed an *in vivo* pooled RNAi screen^{32,33} targeting *Hmgcr* and downstream components of the mevalonate pathway (**Supplementary Fig. 5a**). LSCe cells were transduced with a lentiviral shRNA pool consisting of shRNAs

targeting eight genes (with a minimum of four different shRNAs per gene) and seven control shRNAs (Supplementary Fig. 5b and Online Methods). After 24 h, we harvested half of the cells and transplanted the other half into sublethally irradiated mice. We harvested the bone marrow of the recipient mice 2 weeks later at leukemia onset and performed massively parallel sequencing of genomic DNA to determine the representation of each shRNA in the leukemia cells after 2 weeks *in vivo* compared to the representation in the cells before transplantation. Consistent with our *in vitro* findings with statins, we observed that multiple shRNAs targeting *Hmgcr* were strongly depleted (≥ 20 -fold relative to control hairpins) at 2 weeks, consistent with a role for HMGCR in propagating leukemia *in vivo* (Fig. 4b, Supplementary Fig. 5c, Supplementary Table 6 and Online Methods).

In addition, shRNAs targeting *Fnta*, the gene encoding the common α -subunit of both geranylgeranyl transferase I and farnesyl transferase (FT), and shRNAs targeting *isoprenylcysteine carboxyl methyltransferase (Icmt)* were strongly depleted *in vivo* (Fig. 4b). Geranylgeranyl transferase I and FT transfer prenylation moieties generated in the mevalonate biosynthetic pathway to CAAX proteins, and *Icmt* processes these moieties, stabilizing the moieties on target proteins³⁴. Accordingly, small-molecule FT inhibitors and geranylgeranyl transferase inhibitors likewise inhibited LSCe cells in the co-culture system to various degrees (Fig. 4b and Supplementary Fig. 5d,e).

Because lovastatin was developed to inhibit the synthesis of cholesterol, its pharmacologic properties have been optimized to achieve high concentrations in the liver but not elsewhere³¹. In particular, bone marrow exposure following oral lovastatin administration to humans and mice is predicted to be low³⁵. To address the effects of lovastatin on LSCe cell leukemogenicity *in vivo*, we performed syngeneic bone marrow transplantation studies following 24-h *ex vivo* exposure of LSCe cell co-cultures to lovastatin or DMSO control. Limiting dilution analysis revealed that all of the mice receiving 500 to 10,000 co-cultured LSCe cells in the DMSO group developed leukemia by 5 weeks, whereas only one animal in the lovastatin group developed leukemia by 11.5 weeks (Fig. 4c).

We next extended the transplantation experiments to HSPCs and LSCe cells co-cultured together using a three-component system. We exposed heterotypic co-cultures containing dsRed⁺ LSCe cells, uncolored CD45.1⁺ HSPCs and GFP⁺ BMSCs to lovastatin or DMSO for 48 h, and then transplanted them en masse with untreated wild-type helper splenocytes (CD45.1⁺ CD45.2⁺) into lethally irradiated CD45.2⁺ recipient animals. We observed that mice transplanted with lovastatin-treated mixed cultures survived substantially longer than the DMSO control mice (Fig. 4d), all of which developed leukemia by 3 weeks. Furthermore, CD45 chimerism analysis revealed that long-term hematopoietic engraftment at 16 weeks of the admixed normal HSPCs was comparable to that of DMSO-treated HSPCs co-cultured without LSCe cells (Supplementary Fig. 5f,g), indicating that lovastatin did not impair normal HSPC function. Taken together, these experiments support the possibility that HMGCR inhibition can selectively target LSCs in the bone marrow niche while preserving normal hematopoiesis.

DISCUSSION

The earliest attempts to screen for anticancer small molecules were conducted in living laboratory animals. Although such approaches are highly physiologic, they are not amenable to high-throughput screening and can only interrogate compounds with favorable pharmacologic properties. More recently, there has been a marked shift toward ultra-high-throughput biochemical screens that lack biological complexity but allow for the low-cost screening of massive numbers of compounds. Though this advanced type of screening has identified new AML therapies such as FLT3 inhibitors³⁶, serendipitous discoveries over 50 years ago remain the

standard of care for treatment of AML (for example, daunorubicin and cytarabine)³⁷.

Experimental models that more faithfully reflect the biological complexity of primary disease may facilitate the discovery of next-generation AML therapeutics. Prior efforts have begun to work toward that goal^{2,38–40} but to date have not brought primary stem-enriched mammalian cancer cells, stromal cell support and stem-associated readouts to bear on high-throughput small-molecule screening. The approach herein reflects an initial effort to integrate these principles and may provide physiologic mimicry while enabling large-scale testing of therapeutic candidates. We note the importance of the follow-up studies in naturally arising, primary human leukemia cells as means to ensure that the findings were generalizable, as the screening system could in principle identify compounds specific to MLL-AF9 or to the ectopic overexpression system. Accordingly, the screening system can be extended to other primary mouse and human leukemia models and can also be scaled to larger collections of compounds. To facilitate similar efforts in other laboratories, we have made the cobblestone area quantification algorithms and image analysis software freely available at http://www.cellprofiler.org/published_pipelines.shtml.

The most interesting class of compounds to emerge from the screen was that which selectively killed malignant cells in a manner not readily observable by conventional cell line screening. The existence of such compounds raises the possibility that the biology modeled here is fundamentally distinct from that modeled by cell lines adapted to long-term *in vitro* culture. Among such compounds are those that killed LSCe cells via an effect on the stroma cells, such as BRD7116. The mechanism by which BRD7116 impairs the stroma's ability to support leukemia cells remains an important question for future study.

Lovastatin, an US Food and Drug Administration-approved drug, was found to preferentially inhibit LSCs compared to normal HSPCs, irrespective of leukemia genotype. Genetic, biochemical and pharmacologic evidence reported here support the notion that lovastatin kills leukemia cells via inhibition of its known target, HMGCR. Notably, the *in vivo* selection against *Hmgcr* shRNAs in leukemia within the native bone marrow niche supports the physiologic relevance of the *in vitro* co-culture system, linking the mechanistic target identified for lovastatin sensitivity *in vitro* to leukemia propagation *in vivo*.

Together, the preclinical observations described herein form a compelling case for statins as potential anti-AML therapeutics. Although the potential for statins to yield anticancer effects has been proposed^{41–43}, studies of their effects on primary LSCs within the context of a supportive microenvironment have not been reported. Importantly, statins as a drug class have been optimized for activity within the liver, consistent with their primary use as cholesterol-lowering agents. The clinical testing of the hypothesis that HMGCR inhibition will result in antileukemia activity in patients will require a drug that achieves concentrations in the bone marrow at or above concentrations observed herein to inhibit mouse and human primary AML cells in co-culture (for example, above the EC₅₀ of ~200 nM for lovastatin). Although bone marrow drug concentrations have not been reported, the highest plasma concentration achieved (C_{\max}) for lovastatin at standard dosing (40 mg daily) is only ~50 nM, with a half-life of 2.9 h³⁵, and would thus not be expected to be efficacious. A phase 1 clinical trial of pravastatin in AML found preliminary evidence of an antileukemia effect, prompting an ongoing phase 2 trial⁴⁴. Notably, pravastatin did not score in our LSCe co-culture assay or in a recently reported model of FLT3-mutated AML⁴⁵, consistent with its well-documented low uptake by nonliver cells³¹.

Thus, the antileukemia potential of mevalonate pathway inhibition has yet to be fully explored, warranting additional clinical studies. Careful measures of bone marrow pharmacokinetics and,

ideally, pharmacodynamic measures of HMGR inhibition should therefore be considered. We do note that a recent epidemiological study found that statin use begun before a cancer diagnosis is associated with reduced cancer-related mortality⁴⁶, but whether this result indicates an effect on tumor cells (versus other beneficial effects on the host) is unknown.

A key future research goal should be to identify the effector molecules whose modification via the HMGR pathway explains the antileukemia effects of statins. One candidate would be farnesylation or geranylation of RAS proteins. Despite promising initial studies with farnesyltransferase inhibitors, it was later found that KRAS and NRAS could remain active via geranylgeranyl transferase-mediated prenylation in the presence of farnesyltransferase inhibitors^{47,48}, most likely explaining their lack of clinical efficacy⁴⁹. Subsequent efforts to simultaneously inhibit both proteins, while highly active against pancreatic cancer cells, proved unacceptably toxic in animals⁵⁰. Importantly, it is possible that the antileukemia effect of statins is explained by a mechanism independent of, or complementary to, RAS prenylation. A systematic assessment of mevalonate-dependent effects will most likely provide key insight into leukemia cell sensitivities.

The statin result reported here is just one example of multiple compounds found to preferentially kill leukemia cells over normal HSPCs. These discoveries reflect the power of bringing more physiologically relevant, complex biology to small-molecule screening for AML. We therefore suggest that the approach of reconstructing tissue-like interactions of primary, heterologous cells should be extended more broadly in the search for new cancer therapeutics.

Received 13 March 2013; accepted 20 September 2013;
published online 27 October 2013

METHODS

Methods and any associated references are available in the [online version of the paper](#).

Accession codes. The Gene Expression Omnibus accession number for the gene expression data reported in this paper is [GSE51033](#).

References

- Konopleva, M., Tabe, Y., Zeng, Z. & Andreeff, M. Therapeutic targeting of microenvironmental interactions in leukemia: mechanisms and approaches. *Drug Resist. Updat.* **12**, 103–113 (2009).
- McMillin, D.W. *et al.* Tumor cell-specific bioluminescence platform to identify stroma-induced changes to anticancer drug activity. *Nat. Med.* **16**, 483–489 (2010).
- Somervaille, T.C. & Cleary, M.L. Identification and characterization of leukemia stem cells in murine MLL-AF9 acute myeloid leukemia. *Cancer Cell* **10**, 257–268 (2006).
- Lapidot, T. *et al.* A cell initiating human acute myeloid leukaemia after transplantation into SCID mice. *Nature* **367**, 645–648 (1994).
- Guzman, M.L. *et al.* Nuclear factor- κ B is constitutively activated in primitive human acute myelogenous leukemia cells. *Blood* **98**, 2301–2307 (2001).
- Costello, R.T. *et al.* Human acute myeloid leukemia CD34⁺/CD38⁻ progenitor cells have decreased sensitivity to chemotherapy and Fas-induced apoptosis, reduced immunogenicity, and impaired dendritic cell transformation capacities. *Cancer Res.* **60**, 4403–4411 (2000).
- Despeaux, M. *et al.* Critical features of FAK-expressing AML bone marrow microenvironment through leukemia stem cell hijacking of mesenchymal stromal cells. *Leukemia* **25**, 1789–1793 (2011).
- Krivtsov, A.V. *et al.* Transformation from committed progenitor to leukaemia stem cell initiated by MLL-AF9. *Nature* **442**, 818–822 (2006).
- Plosker, G.L. & Faulds, D. Epirubicin. A review of its pharmacodynamic and pharmacokinetic properties, and therapeutic use in cancer chemotherapy. *Drugs* **45**, 788–856 (1993).
- Stentoft, J. The toxicity of cytarabine. *Drug Saf.* **5**, 7–27 (1990).
- Terpstra, W. *et al.* Long-term leukemia-initiating capacity of a CD34⁺ subpopulation of acute myeloid leukemia. *Blood* **87**, 2187–2194 (1996).
- Breems, D.A., Blokland, E.A., Neben, S. & Ploemacher, R.E. Frequency analysis of human primitive haematopoietic stem cell subsets using a cobblestone area forming cell assay. *Leukemia* **8**, 1095–1104 (1994).

- Ploemacher, R.E., van der Sluijs, J.P., van Beurden, C.A., Baert, M.R. & Chan, P.L. Use of limiting-dilution type long-term marrow cultures in frequency analysis of marrow-repopulating and spleen colony-forming hematopoietic stem cells in the mouse. *Blood* **78**, 2527–2533 (1991).
- Corral, J. *et al.* An MLL-AF9 fusion gene made by homologous recombination causes acute leukemia in chimeric mice: a method to create fusion oncogenes. *Cell* **85**, 853–861 (1996).
- Carpenter, A.E. *et al.* CellProfiler: image analysis software for identifying and quantifying cell phenotypes. *Genome Biol.* **7**, R100 (2006).
- Jones, T.R. *et al.* Scoring diverse cellular morphologies in image-based screens with iterative feedback and machine learning. *Proc. Natl. Acad. Sci. USA* **106**, 1826–1831 (2009).
- Schreiber, S.L. Target-oriented and diversity-oriented organic synthesis in drug discovery. *Science* **287**, 1964–1969 (2000).
- Hassane, D.C. *et al.* Discovery of agents that eradicate leukemia stem cells using an in silico screen of public gene expression data. *Blood* **111**, 5654–5662 (2008).
- Guzman, M.L. *et al.* The sesquiterpene lactone parthenolide induces apoptosis of human acute myelogenous leukemia stem and progenitor cells. *Blood* **105**, 4163–4169 (2005).
- Guzman, M.L. *et al.* An orally bioavailable parthenolide analog selectively eradicates acute myelogenous leukemia stem and progenitor cells. *Blood* **110**, 4427–4435 (2007).
- Escuin, D. *et al.* The hematopoietic-specific β 1-tubulin is naturally resistant to 2-methoxyestradiol and protects patients from drug-induced myelosuppression. *Cell Cycle* **8**, 3914–3924 (2009).
- Memon, R.A. *et al.* Up-regulation of peroxisome proliferator-activated receptors (PPAR- α) and PPAR- γ messenger ribonucleic acid expression in the liver in murine obesity: troglitazone induces expression of PPAR- γ -responsive adipose tissue-specific genes in the liver of obese diabetic mice. *Endocrinology* **141**, 4021–4031 (2000).
- Gimble, J.M. *et al.* Peroxisome proliferator-activated receptor- γ activation by thiazolidinediones induces adipogenesis in bone marrow stromal cells. *Mol. Pharmacol.* **50**, 1087–1094 (1996).
- Wolins, N.E. *et al.* OP9 mouse stromal cells rapidly differentiate into adipocytes: characterization of a useful new model of adipogenesis. *J. Lipid Res.* **47**, 450–460 (2006).
- Naveiras, O. *et al.* Bone-marrow adipocytes as negative regulators of the haematopoietic microenvironment. *Nature* **460**, 259–263 (2009).
- Subramanian, A. *et al.* Gene set enrichment analysis: a knowledge-based approach for interpreting genome-wide expression profiles. *Proc. Natl. Acad. Sci. USA* **102**, 15545–15550 (2005).
- Mootha, V.K. *et al.* PGC-1 α -responsive genes involved in oxidative phosphorylation are coordinately downregulated in human diabetes. *Nat. Genet.* **34**, 267–273 (2003).
- Park, D.J., Vuong, P.T., de Vos, S., Douer, D. & Koeffler, H.P. Comparative analysis of genes regulated by PML/RAR α and PLZF/RAR α in response to retinoic acid using oligonucleotide arrays. *Blood* **102**, 3727–3736 (2003).
- Huntly, B.J. *et al.* MOZ-TIF2, but not BCR-ABL, confers properties of leukemic stem cells to committed murine hematopoietic progenitors. *Cancer Cell* **6**, 587–596 (2004).
- Moore, M.A., Dorn, D.C., Schuringa, J.J., Chung, K.Y. & Morrone, G. Constitutive activation of Flt3 and STAT5A enhances self-renewal and alters differentiation of hematopoietic stem cells. *Exp. Hematol.* **35**, 105–116 (2007).
- Gazzerro, P. *et al.* Pharmacological actions of statins: a critical appraisal in the management of cancer. *Pharmacol. Rev.* **64**, 102–146 (2012).
- Meacham, C.E., Ho, E.E., Dubrovsky, E., Gertler, F.B. & Hemann, M.T. *In vivo* RNAi screening identifies regulators of actin dynamics as key determinants of lymphoma progression. *Nat. Genet.* **41**, 1133–1137 (2009).
- Luo, B. *et al.* Highly parallel identification of essential genes in cancer cells. *Proc. Natl. Acad. Sci. USA* **105**, 20380–20385 (2008).
- Konstantinopoulos, P.A. & Papavassiliou, A.G. Multilevel modulation of the mevalonate and protein-prenylation circuitries as a novel strategy for anticancer therapy. *Trends Pharmacol. Sci.* **28**, 6–13 (2007).
- Bellosta, S., Paoletti, R. & Corsini, A. Safety of statins: focus on clinical pharmacokinetics and drug interactions. *Circulation* **109**, III50–III57 (2004).
- Langdon, W.Y. FLT3 signaling and the development of inhibitors that target FLT3 kinase activity. *Crit. Rev. Oncog.* **17**, 199–209 (2012).
- Weiss, R.B. The anthracyclines: will we ever find a better doxorubicin? *Semin. Oncol.* **19**, 670–686 (1992).
- Gupta, P.B. *et al.* Identification of selective inhibitors of cancer stem cells by high-throughput screening. *Cell* **138**, 645–659 (2009).
- Yeh, J.R. *et al.* Discovering chemical modifiers of oncogene-regulated hematopoietic differentiation. *Nat. Chem. Biol.* **5**, 236–243 (2009).
- Sachlos, E. *et al.* Identification of drugs including a dopamine receptor antagonist that selectively target cancer stem cells. *Cell* **149**, 1284–1297 (2012).
- Dimitroulakos, J. *et al.* Increased sensitivity of acute myeloid leukemias to lovastatin-induced apoptosis: a potential therapeutic approach. *Blood* **93**, 1308–1318 (1999).

42. Li, H.Y., Appelbaum, F.R., Willman, C.L., Zager, R.A. & Banker, D.E. Cholesterol-modulating agents kill acute myeloid leukemia cells and sensitize them to therapeutics by blocking adaptive cholesterol responses. *Blood* **101**, 3628–3634 (2003).
43. Osmak, M. Statins and cancer: current and future prospects. *Cancer Lett.* **324**, 1–12 (2012).
44. Kornblau, S.M. *et al.* Blockade of adaptive defensive changes in cholesterol uptake and synthesis in AML by the addition of pravastatin to idarubicin + high-dose Ara-C: a phase 1 study. *Blood* **109**, 2999–3006 (2007).
45. Williams, A.B. *et al.* Fluvastatin inhibits FLT3 glycosylation in human and murine cells and prolongs survival of mice with FLT3/ITD leukemia. *Blood* **120**, 3069–3079 (2012).
46. Nielsen, S.F., Nordestgaard, B.G. & Bojesen, S.E. Statin use and reduced cancer-related mortality. *N. Engl. J. Med.* **367**, 1792–1802 (2012).
47. Whyte, D.B. *et al.* K- and N-Ras are geranylgeranylated in cells treated with farnesyl protein transferase inhibitors. *J. Biol. Chem.* **272**, 14459–14464 (1997).
48. Rowell, C.A., Kowalczyk, J.J., Lewis, M.D. & Garcia, A.M. Direct demonstration of geranylgeranylation and farnesylation of Ki-Ras *in vivo*. *J. Biol. Chem.* **272**, 14093–14097 (1997).
49. Berndt, N., Hamilton, A.D. & Sebt, S.M. Targeting protein prenylation for cancer therapy. *Nat. Rev. Cancer* **11**, 775–791 (2011).
50. Lobell, R.B. *et al.* Evaluation of farnesyl:protein transferase and geranylgeranyl:protein transferase inhibitor combinations in preclinical models. *Cancer Res.* **61**, 8758–8768 (2001).

Acknowledgments

We wish to thank L. VerPlank, V. Raksakulthai, A. Liberzon, M. Palmer, G. Cowley, J. Burbank, P. Aspesi Jr., M. Bliss-Moreau, D. Barker, B. Wagner, A. Krivtsov, S.A. Armstrong, R. Karmacharya, J. Perez, R. Onofrio, D. Thomas, R. Busanelli, D. Auclair, K. Masson, J. Du, C. Moore, M. Kharas, Y. Hoshida, D. Bachovchin, A. Mullally, J. Grabarek, A. Fraser, A. Basu, J. Cheah, N. Bodycombe, C. Mulrooney,

S. Johnston, G. Walzer, D. Wilpitz, A. Bracha, A. Fabian, C. Hon, J. McGrath, C. Hartland, M. Hickey, T.R. Jones, M. Bray, K. Sokolnicki, R. Okabe, M. Paktinat, M. McConkey, L. Gaffney, L. Solomon, K. Rose and Broad Compound Management. We also thank the Golub, Gilliland and Ebert laboratories for scientific discussions and technical expertise. This work was funded by grants from the Starr Cancer Consortium (SCC Award 11-A50), the US National Institutes of Health (U54CA112962, U01HL1004402, T32 HL007623, T32 GM007753, N01-CO-12400, R01 GM089652, RL1CA133834, 20XS139, RL1HG004671, RL1CA133834, RL1GM084437 and UL1RR024924) and the US National Science Foundation (DBI 1148823). The content of this publication is solely the responsibility of the authors and does not necessarily reflect the views or policies of the Department of Health and Human Services, nor does mention of trade names, commercial products or organizations imply endorsement by the US Government. T.R.G., D.G.G. and S.L.S. are investigators at the Howard Hughes Medical Institute.

Author contributions

A.E.C., A.F.S., A.L.S., A.M.S., B.L.E., D.G.G., D.T.S., K.A.H., M.A.S.M., P.G.M., S.L.S., S.M. and T.R.G. designed the project strategy and interpreted results. A.E.C., A.L.S., A.M.S., D.G.G., D.J.L., D.T.S., J.A.B., J.E.H., J.M.N., K.A.H., N.J.T., P.G.M., S.L.S., S.M., S.S., T.H., T.K. and Z.T. developed the assay. A.L.S., D.J.L., J.A.B., J.M.N., K.A.H., M. Duvet, N.J.T., P.A.C., P.G.M., S.C., S.S. and T.H. conducted small-molecule screening. A.L.S., A.R.K., B.M., C.H., D.J.L., D.P.S., F.A.-S., J.A.B., J.H.S., J.M.N., K.A.H., L.P.C., M. Dai, M. Duvet, M.J., N.J.T., P.G.M., R.N., R.P., S.C., S.S., T.H. and V.D. conducted follow-up studies. A.M.S., B.L.E., K.A.H., P.G.M. and T.R.G. drafted the paper.

Competing financial interests

The authors declare no competing financial interests.

Additional information

Supplementary information and chemical compound information is available in the [online version of the paper](#). Reprints and permissions information is available online at <http://www.nature.com/reprints/index.html>. Correspondence and requests for materials should be addressed to T.R.G.

ONLINE METHODS

Mouse maintenance and transplantation. All of the mouse experiments were in accordance with an Institutional Animal Care and Use Committee-approved animal protocol. Recipient mice were either sublethally (1×5.5 Gy (550 rads)) or lethally irradiated (2×5.5 Gy (550 rads)) before tail vein transplantation. Transplanted cells were rinsed and resuspended in 500 μ l Hank's balanced salt solution (HBSS) and loaded into 27.5-gauge syringes. Leukemia onset was assessed daily.

LSCe leukemia cells and normal HSPCs. To generate LSCe cells, the *MLL-AF9* fusion (kindly provided by S.A. Armstrong at Harvard Medical School and currently at Memorial Sloan-Kettering Cancer Center) was retrovirally transduced as described⁵¹ into primary granulocyte-monocyte progenitors (GMPs; Lin^{lo}, Sca-1, c-Kit⁺, Fc γ RII^{hi} and CD34^{hi}) isolated from β -actin-dsRed transgenic mice (6051, Jackson Laboratory) containing a Red Fluorescent Protein gene (DsRed.MST) under the control of the chicken β -actin promoter coupled with the cytomegalovirus (CMV) immediate early enhancer, accompanied by polyadenylation sites. The cells were then transplanted into wild-type C57BL/6 mice, and the resulting primary leukemias were serially transplanted through secondary, tertiary and quaternary recipient mice, yielding large numbers of LSCe cells with a predictable disease latency. Cell staining was performed using mouse antibodies for CD3 (14-0032-86, eBioscience, 1:15), CD4 (MCD0400, Caltag, 1:30), CD8 (16-0081-85, eBioscience, 1:30), Gr-1 (RM3000, Caltag, 1:15), B220 (RM2600, Caltag, 1:15), CD19 (RM7700, Caltag, 1:30), IL-7R (555288, BD Pharmingen, 1:30) and Ter119 (14-5921-85, eBioscience, 1:15) (all biotin-tagged), as well as Streptavidin-APC γ 7 (554063, BD Pharmingen, 1:30), c-Kit (17-1172-83, eBioscience, 1:200), Sca-1 (11-5981-82, eBioscience, 1:30), CD34 (11-0341-85, eBioscience, 1:30) and Fc γ RII (25-01610-82, eBioscience, 1:30) and Hoechst 33258 viability reagent (Invitrogen). For assay development, LSCe cells were isolated using a Hoechst⁻ dsRed⁺ Lin^{lo} Sca-1⁻ c-Kit^{top 5%} Fc γ RII^{hi} CD34^{hi} gating strategy with the c-Kit gate expanded to c-Kit^{top 10–20%} during primary screening as described¹. As all of the dsRed⁺ leukemia cells in the quaternary transplants were Lin^{lo} and Sca-1⁻ and nearly all of the dsRed⁺ c-Kit^{hi} cells fell into the Fc γ RII^{hi} CD34^{hi} gate, a simplified Hoechst⁻ dsRed⁺ c-Kit^{top 5%} gating strategy was used for further experiments, with the c-Kit gate expanded to c-Kit^{top 10–20%} during primary screening. This same gating strategy was used for the comparison of c-Kit^{hi} and c-Kit^{lo} cells in co-culture, with the c-Kit gate set as c-Kit^{top 25%} and c-Kit^{bottom 25%}, respectively.

Normal HSPCs (DsRed⁺ Lin^{lo} Sca-1⁺ c-Kit⁺ CD48⁻) were isolated from β -actin-dsRed mouse bone marrow (fully backcrossed to the C57BL/6J background) using biotin-conjugated anti-mouse lineage antibodies CD4 (553728, BD Bioscience, 1:100), CD8 (553029, BD Bioscience, 1:100), CD3 (553060, BD Bioscience, 1:100), B220 (55086, BD Bioscience, 1:100), Gr-1 (553125, BD Bioscience, 1:100), Mac-1 (553309, BD Bioscience, 1:100), Ter-119 (553672, BD Bioscience, 1:100) and CD48 (HM48-1, eBioscience, 1:300) and Dynabead magnetic separation (Invitrogen) per the manufacturer's protocol. The resulting Lin/CD48-depleted cells were stained with streptavidin APC-Cy7 (405208, BioLegend, 1:100), c-Kit-APC (2b8, eBioscience, 1:100), Sca-1-FITC (11-5981-82, eBioscience, 1:100) and CD48-Pacific Blue (103417, BioLegend, 1:100) antibodies. A Lin^{lo} Sca-1⁺ c-Kit⁺ (LSK) gating was used for secondary studies using HSPCs from CD45.1 or GFP⁺ mice. FACS plots were created using FlowJo software (Tree Star, Inc).

High-throughput co-culture assay methods. These methods are described in **Supplementary Note 1**.

Human CAFC assays. Cells were obtained from bone marrow and/or peripheral blood of AML patients with informed consent obtained under the procedures of the Memorial Sloan-Kettering Institutional Review Board during initial presentation of disease ('primary') or at relapse ('therapy-related'). Normal cord blood was obtained from the New York Blood Center. Mutations and cytogenetic abnormalities were determined via fluorescence *in situ* hybridization (FISH), karyotyping and DNA sequencing (FLT3, NPM1, CEPB α , KIT). Samples were centrifuged over Ficoll-Paque PLUS (GE Healthcare) step gradients (2,000g for 30 min), yielding mononuclear cells, and then CD34⁺ cells were isolated using immunomagnetic beads (MACS Cell Separation, Miltenyi Biotec), except for the NPM1 mutation sample, which was found to be CD34⁺ by flow cytometry. MS-5 mouse bone marrow-derived stromal cells (kindly provided by K. Itoh, Niigata University) were

plated in 96-well format (20,000 per well in α -MEM containing 10% FCS) and kept at 37 °C/5% CO₂. One day later, CD34-enriched cells (normal or leukemic) were added in 100 μ l of fresh co-culturing medium at a density determined to generate one cobblestone per well after 5 weeks in neutral control wells. The following day, 50 μ l medium containing drug in DMSO was added to each well for a final DMSO concentration of 0.2%. Six days later, the wells were rinsed, and fresh DMSO medium was added. The co-cultures were then maintained with one subsequent half-medium change at 3 weeks and assessed for cobblestones at 5 weeks (2 weeks for FLT3-ITD sample⁵²). A cobblestone was defined as an instance of at least six tightly packed cells beneath the MS-5 stromal monolayer⁵³. The co-culture medium formulation consisted of α -Eagle's minimum essential medium, 12.5% FCS (S11550, Atlanta Biologicals), 12.5% horse serum (Gemini Bio Products), 200 mM glutamine, 1 mM monothioglycerol (Sigma Cell Culture), 1 μ M hydrocortisone (Sigma) and 20 ng/ml human recombinant IL-3 (Amgen).

OP9 and primary mouse BMSCs. OP9 stromal cells (ATCC) were transduced with (GFP)-labeled by retrovirus and cultured in α -MEM without nucleosides (500 mL, 36453, Stem Cell Technologies) with sodium bicarbonate (14.6 mL, 25080-094, Gibco), L-glutamine (5 mL, 071000, StemCell Technologies), β -mercaptoethanol (2.5 mL, ES-007-E, Chemicon International), FBS (100 mL) and penicillin/streptomycin (Pen-Strep). OP9 cells were maintained at low-to-medium density at 37 °C/5% CO₂ and periodically replaced with new stocks to ensure optimal LSCe support. 'OP9 conditioned medium' was isolated from OP9 cells grown for 3 d.

Primary CD105⁺ bone marrow stromal cells were isolated from actin-GFP or ubiquitin C-GFP (000329 or 4353, Jackson Labs) or wild-type C57BL/6 mice. Crushed bones were washed in 0.5% FBS (HyClone) in PBS without magnesium and calcium (Gibco), passed through a 70- μ m filter, subjected to red blood cell lysis with ACK buffer (Lonza) for 3–4 min, and then resuspended in 'BMSC medium' (400 mL α -MEM (StemCell Technologies), 100 mL FBS (HyClone) and 5 mL Pen-Strep). Cells were seeded into 150-cm² tissue culture flasks (25 ml medium volume each, three flasks per mouse) and placed in a 33 °C/5% CO₂ incubator for 2–3 d, and then a medium change was performed. 8–14 d later, the cultures were rinsed, split by brief trypsinization (0.25%), pooled, filtered through a 70- μ m filter, replated at 3–4 million cells per 150-cm² tissue culture flask and grown another 3–4 d until nearly confluent. The cells were then trypsinized, filtered and resuspended in 0.5% FBS in PBS with biotin-conjugated anti-mouse CD105 antibody (13-1051-85, eBioscience, 1:100) for 15–30 min and isolated using Dynabead M-280 streptavidin-linked magnetic beads (Invitrogen) for 15–30 min at 4 °C with agitation and rinsed once. The CD105⁺ cell fraction was replated at 1–2 million cells per 150-cm² tissue-culture flask and incubated at 33 °C/5% CO₂ for 2–3 d before being used for short-term experimentation.

96-well assay setup for secondary studies. For 96-well format secondary studies, GFP⁺ OP9 cells (13,500 per well) were plated onto gelatin-coated 96-well plates (3904, Corning). 24 h later, the medium was removed, 2,000 sorted LSCe cells were added in 100 μ l of OP9 co-culture cocktail medium, 50 μ l of medium containing compound (or compounds) was added approximately 24 h later to a 0.2% final DMSO working concentration, and then a full medium change and compound re-addition were performed 3 d later. For 96-well BMSC co-cultures, 16,000 BMSCs were plated onto fibronectin-coated 96-well plates in 100 μ l BMSC medium. Three days later, 2,000 leukemia cells were plated in 50 μ l BMSC medium and added to the existing medium in each well. The following day, compounds were added in 20 μ l medium and incubated for 5 d. For both types of stroma, the plates were imaged at 4 \times or 10 \times magnification at the completion of 5 d of total compound exposure (6 d of LSCe co-culture). Total viable leukemia cells were counted using the Cell Scoring Application Module in MetaXpress software (Molecular Devices).

Stromal toxicity screen. OP9 or BMSC stromal cells were plated in white-bottom, 384-well plates (6,750 or 2,000 cells respectively; 3570, Corning). After 24 h, compounds were added (eight concentrations), the plates were incubated for 72 h at 37 °C/5% CO₂, and viability was quantified using a luminescence measure of cellular ATP (CellTiter-Glo, Promega). 36 compounds were removed from the 196 tested owing to stromal toxicity at concentrations below 20 μ M (mean signal \leq 3 s.d. below DMSO control with BMSCs, 5 s.d. with OP9s).

Selectivity retesting of LSCe co-culture and HSPC co-culture effects. The remaining 155 prioritized compounds were tested (8–12 concentrations) in duplicate on LSCe cells in 384-well format (300 per well) and on HSPCs (400 cells per well) with BMSCs at 33 °C/5% CO₂. One subset was retested on LSCe cells with BMSCs using freshly sourced compound, and another subset (**Table 1**) was retested on HSPCs with BMSCs at eight concentrations. Compounds prioritized during these steps were selected on the basis of the degree of selectivity relative to HSPCs, potency of LSCe cell effects and novelty. BRD2761 (5-chloro-7-((4-ethylphenyl)(pyridin-2-ylamino)methyl)quinolin-8-ol) at 22 μM was used as a positive control for HSPC toxicity.

Human AML cell line viability screens. Human AML cell lines (ATCC) were cultured under standard conditions in medium specified by ATCC. 3,000 cells in 30 μL were plated into 384-well plates. 16 h later, 100 nL of compounds in DMSO were added, and the plates were incubated at 37 °C/5% CO₂ for 72 h and then analyzed using CellTiter-Glo. A two-point normalization was performed per screening plate using the mean of DMSO wells (set at 0% effect) and the mean of the cytotoxic positive control wells (0.4 μM staurosporine, set at –100% effect). The independent cell line viability screen was performed as described³⁴. Cells were plated at an optimal density determined during assay development in 384-well format and incubated overnight at 37 °C/5% CO₂. Compounds were pin-transferred into duplicate assay plates and incubated for 72 h. Cellular viability was assessed using CellTiter-Glo.

Stromal pretreatment screen. OP9 cells were plated into monolayers in 384-well plate format, as in the original co-culture screen. 24 h later, 100 nL of compounds in pure DMSO at various concentrations were added, the plates were incubated at 37 °C/5% CO₂ for 3 d, the wells were washed twice with PBS to a 600-fold dilution, and then LSCe cells were plated. Medium was changed 3 d later, and the plates were imaged and analyzed 2 d after that. Notably, the pretreatment assay may underestimate the cell-non-autonomous effect of the compound on LSCe cells. Medium conditioned by untreated OP9 cells was added to support the leukemia cells at the time of LSCe cell plating, as required for efficient cobblestone area formation, potentially restoring stromally secreted factors affected by pretreatment.

For the pretreatment studies using primary BMSC stroma, GFP⁺ HSPCs (from UbiquitinC-GFP mice) and LSCe cells (dsRed⁺) were plated together (1,200 HSPCs, 1,200 LSCe cells, each in 25 μL medium) in 384-well format onto BMSC stromal monolayers (isolated from wild-type C57BL/6 mice) that were previously treated with BRD7116 for the 3 d prior at 33 °C/5% CO₂. The treated monolayers were rinsed twice with PBS before the plating of the hematopoietic cells. 5 d later, the wells were imaged in the dsRed and GFP channels at 10× magnification, and total cell areas (per well) in each channel were quantified using MetaXpress software.

Compounds. Compounds screened are listed in **Supplementary Table 2**. Compounds were diluted to a final working concentration of 0.2% DMSO. Sources of compounds are described in **Supplementary Table 3**. Lovastatin was purchased from Analyticon Discovery (lovastatic acid, NP-001236; primary, retest and secondary screens) and Sequoia Research Products (lovastatin, SRP015851; secondary experiments). The top 155 compounds (**Supplementary Table 3**) were picked for high-throughput screening from Broad small-molecule libraries and were ≥75% pure. For secondary studies, we determined the purity of BRD7116 and lovastatin to be greater than 99% pure, with lovastatin existing as an 80/20 mixture of the closed prodrug and free acid forms. Tandem LC/MS was performed on a Waters 2795 separations module and 3100 mass detector. Compound purity was determined by monitoring UV absorbance at 210 nm, followed by detection of the expected molecular ion.

Gene expression analysis. RNA was extracted (RNeasy kit 74104, Qiagen) from 250,000 LSCe cells treated with either 5 μM BRD7116 or DMSO control ($n = 5$ and 2 , respectively) for 6 h in suspension in 150 μL of IMDM, 10% FBS and 1% Pen-Strep and prepared (Illumina TotalPrep 96 RNA Amplification Kit, Applied Biosystems, PN no. 4393543) for hybridization to Illumina's MouseRef-8 v2.0 Expression BeadChip per the manufacturer's protocol. Illumina's BeadArray Reader was used to measure the fluorescence intensity at each addressed bead location, according to the manufacturer's instructions. Raw data were normalized using the cubic spline method implemented in the Illumina Normalizer module of the GenePattern analysis tool kit

(<http://www.broadinstitute.org/cancer/software/genepattern/>) and converted into human gene symbols on the basis of the orthologous gene mapping table provided by Jackson Laboratory (<http://www.jax.org/>). For each compound, a ranked list of genes was created by comparing the treated samples to DMSO control samples. The genes were ordered using the signal-to-noise statistic (the difference of means in each group scaled by the sum of s.d., computed over three treatment replicates). The ranked lists were analyzed using GSEA³⁶ at <http://www.broadinstitute.org/gsea/index.jsp>.

Other statistics. Statistical significance was assessed using the two-tailed Student's *t*-test (two-sample, assuming unequal variances) in Excel (Microsoft). *P* values were as stated in figure legends, where 'not significant' indicates a *P* value greater than 0.09. Kaplan-Meier survival analysis was performed using the log-rank (Mantel-Cox) test in Prism 5 (GraphPad). All other statistical analysis was performed with R (<http://www.r-project.org/>) or Excel, except where noted. All of the averages were calculated as means unless otherwise noted, with error bars denoting s.e.m.

Murine myeloid cell line studies. The mouse myeloid cell lines (all from ATCC) were maintained as specified by ATCC at 37 °C/5% CO₂. Each line was plated under standard conditions in 96-well format (15,000 cells per well in 150 μL medium). 18 h later, 20 μL of medium containing lovastatin or DMSO to a final DMSO concentration of 0.2% was added. 72 h later, cellular viability was assessed using CellTiter-Glo reagent. The assay was also read at 5 d with no apparent shift in EC₅₀ observed.

MOZ-TIF2 LSCe cell co-culture studies. Primary MOZ-TIF2 LSCe cells were generated and isolated as described³⁹ as for MLL-AF9 LSCe cells but with one additional round of transplantation. Viable MOZ-TIF2 cells within BMSC (GFP⁺) co-cultures were quantified after trypsinization using flow cytometry and counting beads (5,000 per well; C36950, Life Technologies). All of the other assay parameters were as described above for MLL-AF9 LSCe cells with BMSCs in 96-well format.

In vitro studies of admixed HSPCs and LSCe cells in co-culture. BMSC monolayers (from C57BL/6 mice) were plated into 384-well plates in 30 μL as described, and then 800 LSCe cells (dsRed⁺) and 1,600 normal HSPCs (GFP⁺; C57BL/6 UbiquitinC-GFP mice) were added 3 d later (in 10 μL medium each). 24 h later, lovastatin (5 μM) or DMSO was added, and the plates were incubated for 5 d, after which the wells were imaged in the dsRed and GFP channels at 10× magnification, and total cell areas (per well) in each channel were quantified using MetaXpress software.

Mevalonate rescue of lovastatin treatment. 96-well co-culture assays of LSCe cells with OP9 stroma were performed as described, with treatment with 2 mM mevalanolactone (M4667, Sigma-Aldrich) and/or 1 μM lovastatin. Both reagents were added simultaneously, and the DMSO carrier concentration was kept constant across all of the wells.

In vivo pooled RNAi screen. Detailed viral packaging protocols for generating arrayed virus for use in pooled shRNA studies can be found at <http://www.broadinstitute.org/rnai/public/resources/protocols/>. In replicates of five, LSCe cells suspended in 400 μL (5 million/ml) in IMDM, 10% FBS, 10 ng/ml mIL-3 (PeproTech), 10 ng/ml mIL-6 (PeproTech), 20 ng/ml BMSCF (PeproTech) and 5 μg/ml polybrene (Sigma-Aldrich) were infected with 400 μL of pooled virus in 12-well plates (spinfection at 2,500 r.p.m., 37 °C for 90 min). Two hours later, 800 μL of fresh IMDM, 10% FBS, 10 ng/ml mIL-3, 10 ng/ml mIL-6 and 20 ng/ml BMSCF was added to each well. After 24 h, each well was split; half of the cells were frozen for processing, and the other half were transplanted into sublethally irradiated mice. Two weeks later, the recipient mice were killed, and bone marrow was harvested for DNA sequencing (QIAamp Blood Mini Kit, Qiagen).

The shRNA region was PCR amplified from the purified genomic DNA by combining 5 μL primary PCR primer mix, 4 μL dNTP mix, 1× Ex Taq buffer, 0.75 μL of Ex TaqDNA polymerase (TaKaRa) and 6 μg genomic DNA in a total reaction volume of 50 μL. Thermal cycler PCR conditions consisted of heating samples to 95 °C for 5 min; 15 cycles of 94 °C for 30 s, 65 °C for 30 s and 72 °C for 20 s and then 72 °C for 5 min. PCR reactions were then pooled by sample. A secondary PCR step was performed containing 5 μM of common barcoded 3' primer, 8 μL dNTP mix, 1× Ex Taq buffer, 1.5 μL Ex TaqDNA

polymerase and 30 μL of the primary PCR mix for a total volume of 90 μL . 10 μL of independent 5' barcoded primers were then added into each reaction, after which the 100 μL total volume was divided into two 50- μL final reactions. Conditions for secondary PCR were: 95 $^{\circ}\text{C}$ for 5 min; 15 cycles of 94 $^{\circ}\text{C}$ for 30 s, 58 $^{\circ}\text{C}$ for 30 s and 72 $^{\circ}\text{C}$ for 20 s and then 72 $^{\circ}\text{C}$ for 5 min. Individual 50- μL reactions were then re-pooled. Reactions were then run on a 2% agarose gel and intensity normalized. Equal amounts of samples were then combined and gel-purified using a 2% agarose gel. Massively parallel sequencing was then performed using a custom sequencing primer under standard Illumina conditions. The raw read counts for each shRNA were normalized to the total reads, and the calculated fold change of normalized reads between the two time points was divided by the mean fold change of all of the control shRNAs over the same time points. A gene scored as a hit if ≥ 2 unique shRNAs specific to that gene had a greater than 20-fold change relative to control shRNAs. The seven control shRNAs used in the pooled *in vivo* RNAi screen, and the gene hits identified in the pooled *in vivo* RNAi screen are shown in **Supplementary Tables 7 and 8**, respectively.

shRNA knockdown efficacy. Ba/F3 cells maintained in RPMI (11875135, Invitrogen) with 10% FBS, 10 ng/mL mouse IL3 (PeproTech), 1 \times Pen-Strep (15140-122, Gibco) and 5 $\mu\text{g}/\text{mL}$ polybrene (Sigma) were spinfected. Three control shRNAs (LUC-58, RFP-03, LacZ-29) were used in addition to the *Hmgcr* shRNAs. 24 h later, puromycin (2 $\mu\text{g}/\text{mL}$, Sigma) was added. The cells were harvested 3 d later. RNA was isolated with a TurboCapture assay (Qiagen) and processed to cDNA using a SensiScript kit (Qiagen). All quantitative PCRs were performed using the Taqman assay (Applied Biosystems) on a 384-well qPCR machine (ABI Prism) with knockdown determined using $\Delta\Delta\text{CT}$ analysis and the *Gapdh* reference gene.

Chemical inhibition of geranylgeranyl and FTIs. Co-culture assays of LSCe cells with OP9 stroma were performed in 96-well format with FTI-277 (10 μM , F9803, Sigma-Aldrich), FTI L744,832 (5 μM , BML-G242, Enzo Life Sciences), GGTI-286 (10 μM , 345878, Calbiochem) and GGTI-298 (10 μM , 345883, Calbiochem), all at 0.2% DMSO.

Syngeneic transplantation experiments. Co-cultures of LSCe cells with BMSCs were plated in 96-well format with 500, 100 or 25 LSCe cells per well.

6 d later, each well was rinsed with PBS, trypsinized and transplanted *en masse* into a sublethally irradiated recipient mouse. For the limiting dilution experiments with and without lovastatin treatment, co-cultures of LSCe cells with BMSC (GFP⁺) stroma were plated with 500 to 10,000 LSCe cells per well and treated with 5 μM lovastatin or DMSO 24 h later. After 5 d, each well was rinsed with PBS, trypsinized and transplanted into a sublethally irradiated recipient mouse.

For the triple co-cultures, BMSC monolayers (GFP⁺) were plated into 96-well plates, and then 10,000 freshly isolated LSCe cells (dsRed⁺) and 10,000 normal HSPCs were added. Lovastatin (5 μM) or DMSO was added 1 d later. 48 h later, the wells were trypsinized and transplanted along with 2 million helper splenocytes from 6-month-old CD45.1⁺ CD45.2⁺ mice into lethally irradiated, CD45.2⁺ recipient mice. Mice were monitored daily for the presence of leukemia, and those that succumbed to leukemia before 16 weeks were killed. The multi-lineage long-term engraftment of the co-cultured HSPCs (CD45.1⁻) was quantified by FACS analysis of the peripheral blood of mice alive after 16 weeks and compared to results from mice that received HSPCs co-cultured with DMSO in the absence of LSCe cells. CD45.1⁺ B, T and myeloid cells were also quantified using FACS. Antibodies include B220 (Ra3-6b2, BD Bioscience, 1:200), CD3 (17A2, eBioscience, 1:100) and Gr-1/CD11b (RB6-8C5, BD Bioscience, 1:200; M1/70, BioLegend, 1:200), CD45.1 (A20, BD Bioscience, 1:100) and CD45.2 (552950, BD Bioscience, 1:100).

51. Krivtsov, A.V. *et al.* Transformation from committed progenitor to leukaemia stem cell initiated by MLL-AF9. *Nature* **442**, 818–822 (2006).
52. Moore, M.A., Dorn, D.C., Schuringa, J.J., Chung, K.Y. & Morrone, G. Constitutive activation of Flt3 and STAT5A enhances self-renewal and alters differentiation of hematopoietic stem cells. *Exp. Hematol.* **35**, 105–116 (2007).
53. van Os, R.P., de Haan, G. & Dethmers-Ausema, B. *In vitro* assays for cobblestone area-forming cells, LTC-IC and CFU-C. *Methods Mol. Biol.* **430**, 143–157 (2008).
54. Basu, A. *et al.* An interactive resource to identify cancer genetic and lineage dependencies targeted by small molecules. *Cell* **154**, 1151–1161 (2013).